Smart Agricultural Technology 9 (2024) 100528

Contents lists available at ScienceDirect

Smart Agricultural Technology

journal homepage: www.journals.elsevier.com/smart-agricultural-technology

Application of computer vision and machine learning in morphological characterization of *Adansonia digitata* fruits

Franklin X. Dono [a,b,c,*], Bernard N. Baatuuwie [a,d], Felix K. Abagale [a], Peter Borgen Sørensen [e]

[a] *West African Center for Water Irrigation and Sustainable Agriculture (WACWISA), University for Development Studies, P.O. Box TL 1882, Tamale, Ghana*
[b] *Department of Environmental Management and Sustainability, University for Development Studies, P.O. Box TL 1882, Tamale, Ghana*
[c] *Ghana Atomic Energy Commission (GAEC), Nuclear Power Institute (NPI), P.O. Box LG 80, Legon, Accra Ghana*
[d] *Department of Natural Resources and Geo-Information Sciences, Faculty of Natural Resources and Environment, University for Development Studies, P.O. Box TL 1882, Tamale, Ghana*
[e] *Institute of Ecoscience, Faculty of Technical Sciences, Aarhus University, C.F. Møllers Allé 4, 8000 Aarhus, Denmark*

ARTICLE INFO

Keywords:
Baobab fruit
Computer vision
Machine learning
Image processing

ABSTRACT

Measuring fruit mass and volume is a time-consuming and tedious task that can affect production planning. This study developed a computer vision system to estimate the volume and mass of baobab fruits from single-view images captured from inexpensive and readily available cameras such as those in smartphones. The baobab fruits were collected from two study fields within the savanna ecological zone. Their images were captured, and subsequently, they were detected and segmented with over 97 % accuracy. The segmented images were binarized, and two-dimensional (2D) features such as the segmented area, centroid, bounding box, equivalent diameter, and major diameter were extracted from them. The volumes of the fruits were estimated from the 2D features using random forest, linear, polynomial, and radial support vector machine models. All the models achieved high goodness of fit; however, the random forest model delivered the best performance, with an R^2 value of 99.8 %. The relationship between mass and volume was a quadratic equation (mass = 38.23 + 0.25 × volume + 4.49e−05 × volume^2) and had an R^2 value of 92 %. Correlations were validated via plots and statistical tests, and credible intervals of point estimates were determined from the posterior distributions of their samples. This highlights the potential of artificial intelligence methods to be applied in a less constrained environmental setting for ecological research and agricultural management. Commercial companies producing baobab powder and seed oil should apply these models for effective production planning. To enhance the model, it would be beneficial to gain a better understanding of how climate gradients affect the morphological characteristics of baobab fruits.

1. Introduction

Native multipurpose tree species within the savanna ecological zone provide numerous ecosystem services [1]. The baobab is one such native multipurpose species found in the savannas of West Africa.

The export value of baobab fruits has increased over the last decade [2–4], and opportunities for African markets have expanded. Despite their economic prospects, not all baobabs are in high demand. According to Odoom [5], fruit size varies from large to small and is an indicator of sweetness. Gurashi and Kordofani [6] associated the shape of the fruit with its market value. Therefore, attributes such as size and shape can affect consumer preference and market value, both of which influence demand. This calls for the selection of suitable varieties for both marketing and propagation. As a result, researchers have intensified studies on the morphology of baobab fruit to gain insight into how it impacts production, quality, and domestication potential [7–9]. Morphological variability in baobab fruit shape in combination with the percentage of pulp weight is a possible criterion for selecting high-yield fruits [1] and Gurashi and Kordofani [6], confirmed this assertion. Despite the usefulness of these findings, measuring the length and width of the fruit and their component weights using hand-operated tape and an electronic scale was manual, laborious, and time-consuming. This problem persists in most studies in industry [6,10,11].

The determination of suitable baobab fruits for domestication and

* Corresponding author at: West African Center for Water Irrigation and Sustainable Agriculture (WACWISA), University for Development Studies, P.O. Box TL 1882, Tamale, Ghana.

E-mail address: frankxdono@gmail.com (F.X. Dono).

https://doi.org/10.1016/j.atech.2024.100528
Received 12 June 2024; Received in revised form 5 August 2024; Accepted 5 August 2024
Available online 6 August 2024

production by analyzing their morphological characteristics requires less labor-intensive methods for efficient and large-scale production. Mass and volume are useful in planning for sorting, storage, packaging, and transport [12,13]. They directly affect storage and transport costs, which influence sales [14]. In agriculture, weight is often used as a proxy for size because of its relative ease of measurement compared with volume, but volume-based sorting is more efficient [15]. Compared with mass, the volume of fruit is less affected by external factors such as moisture content. Because of the complexity associated with measuring the volume of irregular objects using geometry, fruit volume is commonly measured by gas or water displacement. Both methods are unsuitable for production because they are best conducted indoors and are time-consuming. In addition, the water displacement method (WDM) can have harmful effects on the quality of the fruit. It is therefore not surprising that information on the volume of baobab fruit is scarce in the literature. A more efficient and less laborious process that is easily scalable and does not compromise fruit quality is needed to measure morphological characteristics.

Object detection is a common and challenging task in computer vision but can be implemented to characterize baobab fruits by their mass and volume. The technique aims to locate instances of object classes in a specific image by color and texture or otherwise [16]. Previously, image processing techniques and computer vision have been effective at extracting the diameter, area, and perimeter of spherical objects [12,17]. In fruit grading or sorting by color, texture, or morphological features, computer vision and regression present an intelligent alternative that can be achieved at scale in a cost-effective and timely manner [18]. In addition to other methods, these methods have been applied to determine the mass and volume of cherry tomatoes in Nanjing, Jiangsu Province, China [14,19], and Thai apple ber, scientifically known as *Ziziphus mauritiana* L., in Jodhpur, India [20].

Food products are classified into axis-symmetric and non-axis-symmetric shapes [21]. Thus, a product can be regarded as an axis-symmetric object if its cross-sections are circular while perpendicular to its major axis [19] and include cherry tomatoes, eggs, watermelons, lemons, limes, oranges, and tangerines. In contrast, axis nonsymmetric fruits have different shapes that are affected by genetics and the environment [12]. In Kordofan, Sudan, Gebauer and Luedeling [1] identified four baobab fruit shapes: ventricose, crescent, globose, and fusiform. Gurashi and Kordofani [6] expanded this classification by identifying nine additional shapes in the Blue Nile and North Kordofan States in Sudan: ellipsoid, high spheroid, ovate, obovate, oblong-pointed, spheroid-emarginate, ellipsoid-pointed, clavate, and rhomboid. Thus, the baobab fruit is an example of an axis nonsymmetric fruit.

Various geometric models and numerical analysis methods have been used to extract volumes from 3D reconstruction of fruits from images obtained from different camera arrangements [15,19,22]. Under the assumptions of axis-symmetric shapes, controlled fruit orientation, uniform lighting, and a simple background, very high levels of accuracy have been achieved using basic solids, solids of revolution, and conical frustum to estimate the mass and volume of fruits [15,22]. Nyalala et al. [19] used a 3D Kinect Infra-Red Sensor, which was invariant to visible light conditions and had capabilities for depth estimation and ease of image segmentation to construct depth images to estimate the volume and mass of tomatoes. However, deviations from the assumption in a production environment can introduce errors in the estimates of the mass and volume of fruits. In addition, the assumptions of axis-symmetric shapes, controlled fruit orientation, uniform lighting, and simple background are difficult to achieve under real-world field conditions. These assumptions can affect the accuracy of the resulting models and their application in real-world situations. For example, Fitriyah [12] reported poor to moderate accuracy when using single frontal view images for non-axis-symmetric shapes.

This study seeks to address the limitations imposed by the assumptions of previous studies. It aims to develop a computer vision system to estimate the volume of non-axis symmetric baobab fruits from single-view RGB images captured in a setting where fruit orientation, lighting, and background are not controlled. The specific objectives are (1) to investigate the variation in fruit morphological characteristics across the study areas, (2) to analyze the Mask Region-based Convolutional Neural Network (Mask R-CNN) and adapt it for the effective segmentation of baobab fruits, (3) to develop a 2D feature extraction algorithm, (4) to develop a model to estimate volume, (5) to investigate the relationship between mass and volume, and (6) to extend point estimates of mass and volume to their distributions. The approach used to estimate the volume of fruits provides insights that can be used to optimize sorting, transportation planning, storage, and market pricing strategies to foster efficiency in production and transactions for sellers and buyers. Knowing the relationship between mass and volume in production planning can facilitate the estimation of storage space for fruits when their mass is known.

2. Materials and methods

2.1. Study area

The study was conducted in the savanna ecological zone of Ghana within the Nandom and Kasena–Nankana East municipalities. The Nandom Municipal is located in the Upper West Region, between Longitudes 2°41′ W and 2°54′ W and Latitudes 10°44′ N and 11°00′ N. The Kasena-Nankana East Municipal is located in the Upper East Region, between Longitudes 1°10′ W and 0°53′ W and Latitudes 10°30′ N and 11°01′ N (Fig. 1). The monthly average temperatures ranged from 21 °C to 32 °C. The municipalities experienced a dry season from November to April and a rainy season from May to September/October [23].

2.2. Study species

Baobab (*Adansonia digitata L.*) plays a vital role, particularly in the food, cosmetic, and pharmaceutical industries [7]. The baobab is a massive deciduous fruit tree, up to 20–30 m high, with a lifespan of several hundred years, and the trunk can be as broad as 3–7 m in diameter [24]. According to Odoom, [5], the fruit has an acidic tar flavor, surpasses spinach in calcium content, and sweet oranges in vitamin C. It is a 35 cm long and 17 cm diameter ovoid capsule with a woody envelope, black seeds, and chalky pulp when ripe [24].

2.3. Tree sampling and fruit collection

A total of 166 baobab fruits were collected from 43 randomly selected trees in the savanna ecological zone of Ghana. Among these fruits, 101 were from 26 trees in the Nandom Municipality (Nandom), and the remaining 65 were from 17 trees in the Kasena Nankana East Municipality (Navrongo). The harvesting techniques outlined by Odoom [5] were used for fruit collection during the harvesting period in February and March. Three to four fruits were collected from the northeastern, southeastern, southwestern or northwestern quadrants of the tree crown.

2.4. Measurement of fruit characteristics

Direct measurements of the volume and mass of the 166 fruits were taken. Each fruit was labeled with the study area code and identification number, which were maintained throughout the measurement process. All the measurements were taken at room temperature. The baobab fruit was weighed to a precision of one gram. It was coated with saran wrap and submerged in water with a sinker rod of negligible volume, and displaced water was collected and weighed. Using the density of water at room temperature, the volume was calculated in cubic centimeters (cm^3). The major lengths and maximum circumferences of the fruits were measured using a flexible tape with 0.10 cm precision.

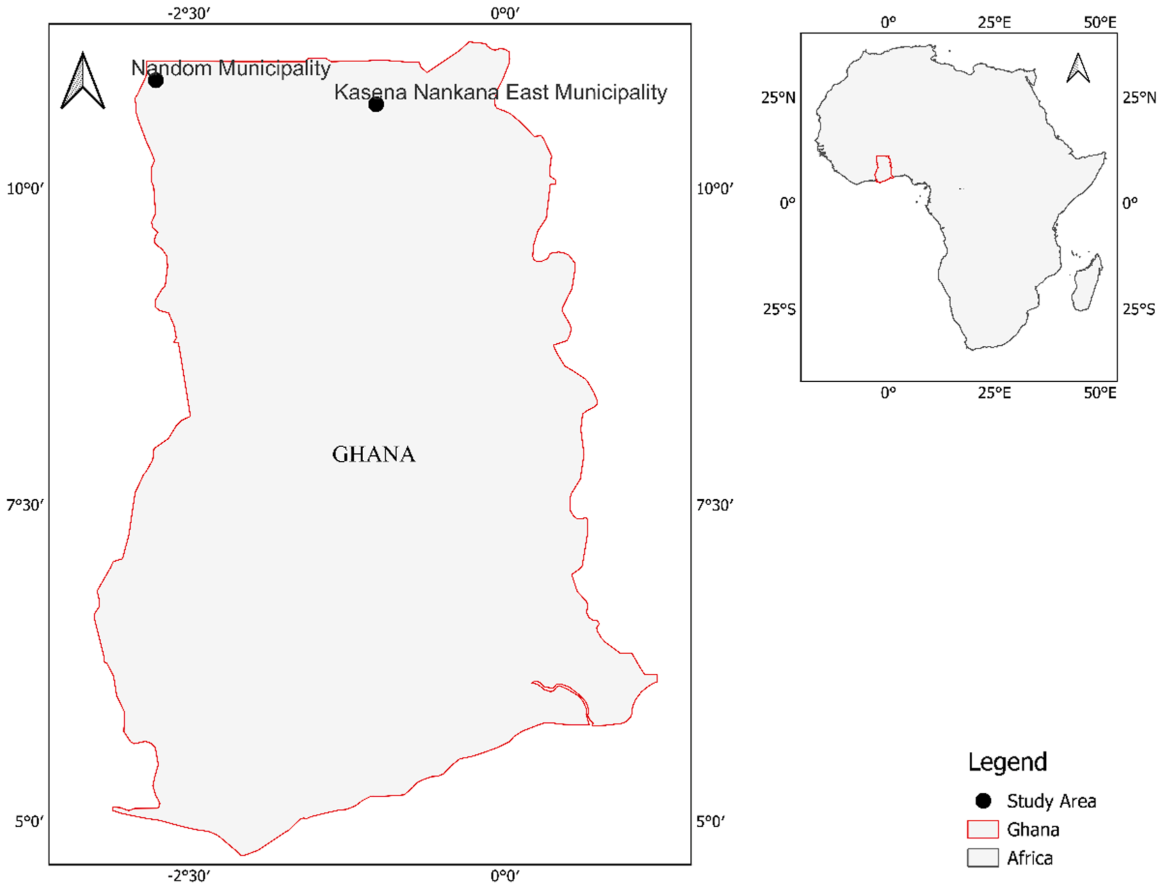

Fig. 1. Study area in Africa within the savanna ecological zone of Ghana.

2.4.1. The computer vision system

The conceptual framework of the proposed system takes an image of the baobab fruit(s) as input. The fruits are detected and segmented (instance segmentation) by a modified Mask R-CNN model to address limitations caused by uncontrolled fruit orientation, shape, lighting, and background. The output is binarized, and two-dimensional (2D) features are extracted to estimate fruit volume or mass when the volume is known. The distribution of the sample is subsequently determined to extend the usefulness of the information from the point estimates for production planning (Fig. 2).

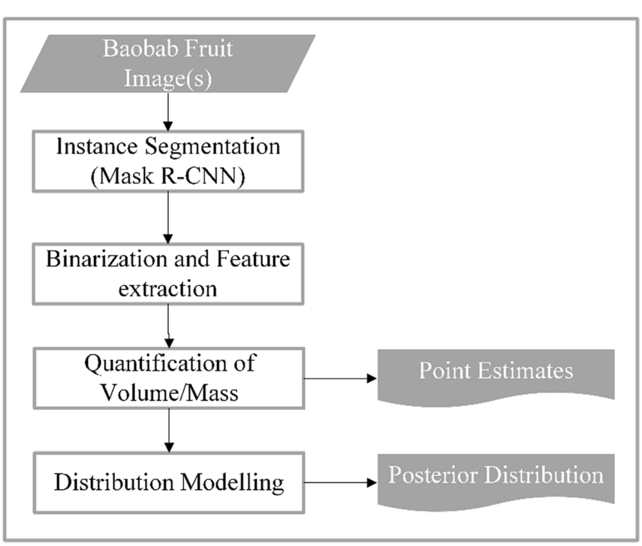

Fig. 2. Conceptual framework of the proposed system.

2.4.2. Instance segmentation

An iPhone XS Max camera with a focal length of 4.25 mm and a resolution of 3024 × 4032 was used to capture all the images. The camera was placed at a fixed distance of 130 cm from the center of a white background with dimensions of 93 cm × 123 cm. Using the Nandom samples, images of different fruit counts were captured and down-sampled to a resolution of 381 × 503 pixels. They were subsequently annotated using the visual image annotator (VIA) by the visual geometry group (VGG) [25]. The annotations were converted to coco-style [26] and split into training (80 %) and testing (20 %) datasets. The datasets were used to fine-tune the Mask R-CNN for detection and instance segmentation (Fig. 3). The ResNet-50 feature pyramid network (FPN) was used as the model backbone, and the initial weights for training were obtained from the Zoo model.

The accuracies of the models were evaluated using loss box regression, loss classification, loss mask, and mask accuracy. Loss box regression measures the model's ability to predict bounding boxes. Loss classification assesses the accuracy of class assignment to detected objects, and a loss mask is used to measure the accuracy of the pixel predictions. Lower values of the loss metrics were preferred. The mask accuracy represents the accuracy of the predicted segmentation mask, and higher values indicate better accuracy.

2.4.3. Image processing and feature extraction

The fruits were grouped by study area, and without consideration of their arrangement relative to each other, they were photographed in groups of 1–25. The images were rotated 360° at 30° intervals and flipped left-to-right and up-to-down. The new dataset was fed into the trained Mask R-CNN model to detect and segment instances of the

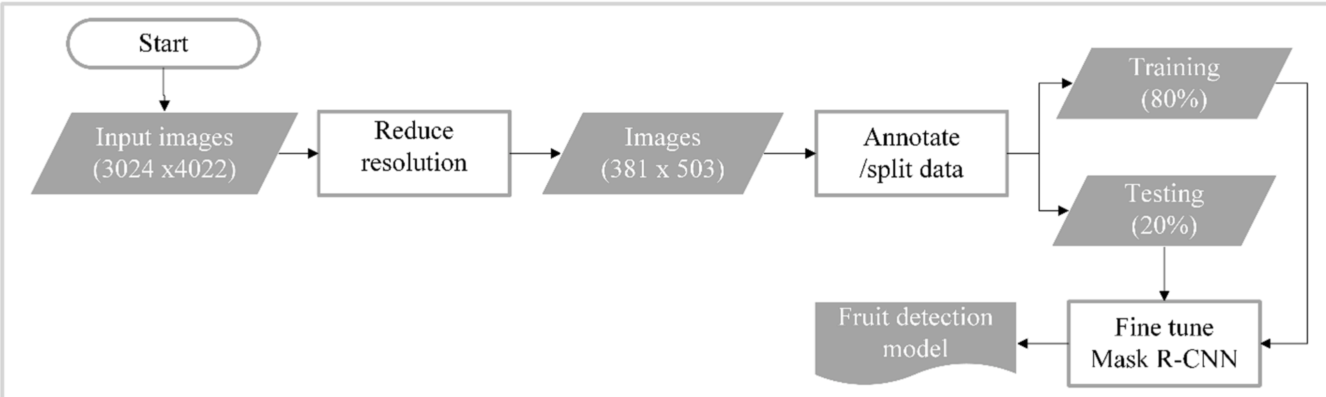

Fig. 3. Training and testing procedure for fruit detection and segmentation.

baobab fruit regions to output a predicted mask image with a unique label assigned to each contiguous region. The predicted masks were converted to binary images of fruits and background and relabeled. The geometric and positional measures were extracted from the relabeled binarized image using scikit-image to measure the region properties. The properties measured included (1) the segmented area, (2) the co-ordinates of the centroid, (3) the coordinates of the bounding box, (4) the equivalent diameter, and (5) the major diameter. The unique labels and extracted measurements of region properties were written to a Comma Separated Value (CSV) file (Fig. 4).

Images with more than one fruit were used to assess the effectiveness of the segmentation process.

2.5. Quantification of volume and mass

The features extracted from single images obtained from Nandom were combined with their corresponding volumes from WDM to train and test the models and, likewise, for records from Navrongo, which were used to validate the results. The CSV data from Section 2.4.3 were filtered for records obtained from single images. They were matched to their corresponding volume measurements from the WDM separated by the study area. The data from Nandom were split into training (70 %) and testing (30 %) and applied to linear, polynomial, and radial implementations of support vector machines (SVMs) and random forest to derive suitable prediction models. The records from Navrongo were used to validate the models (Fig. 5). The results were evaluated using the mean average error (MAE), root mean square error (RMSE), and R-squared (R^2) values.

2.5.1. Statistical analysis

A paired t test and the mean difference confidence interval approach were used to compare the volumes determined by each model (support vector machine and random forest) on the validation dataset with the volumes from the water displacement method. The Bland and Altman [27] approach was used to plot the agreement between the Baobab fruit volume measured by the water displacement method and machine learning quantifications. The statistical analyses were performed in R.

2.6. Modeling probability density functions

The bootstrap resampling technique was used with the distribution fitting package in R to estimate the probability density function for the sampling distribution of the means and standard deviations of fruit mass, volume, and density. The Akaike information criterion (AIC) and Bayesian information criterion (BIC) were used to select the best fit of the normal, exponential, gamma, logistic, Cauchy, Weibull, and log-

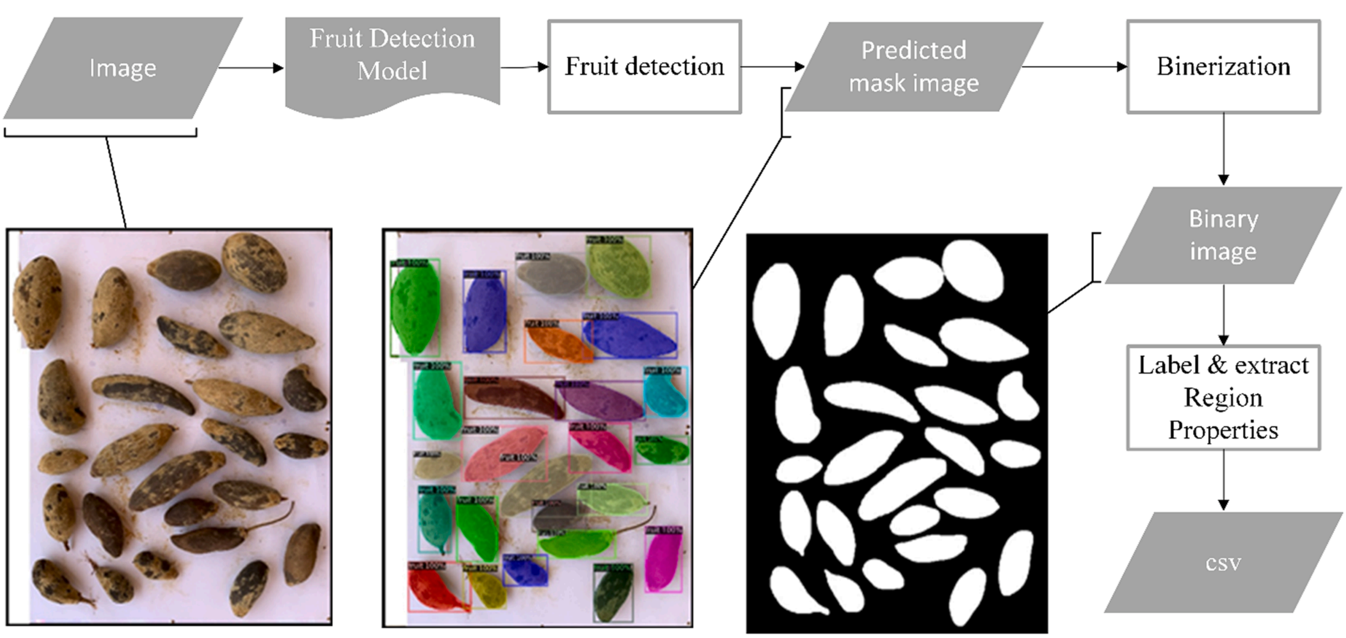

Fig. 4. Instance segmentation of an image of baobab fruits to produce a predicted mask image for two-dimensional feature extraction.

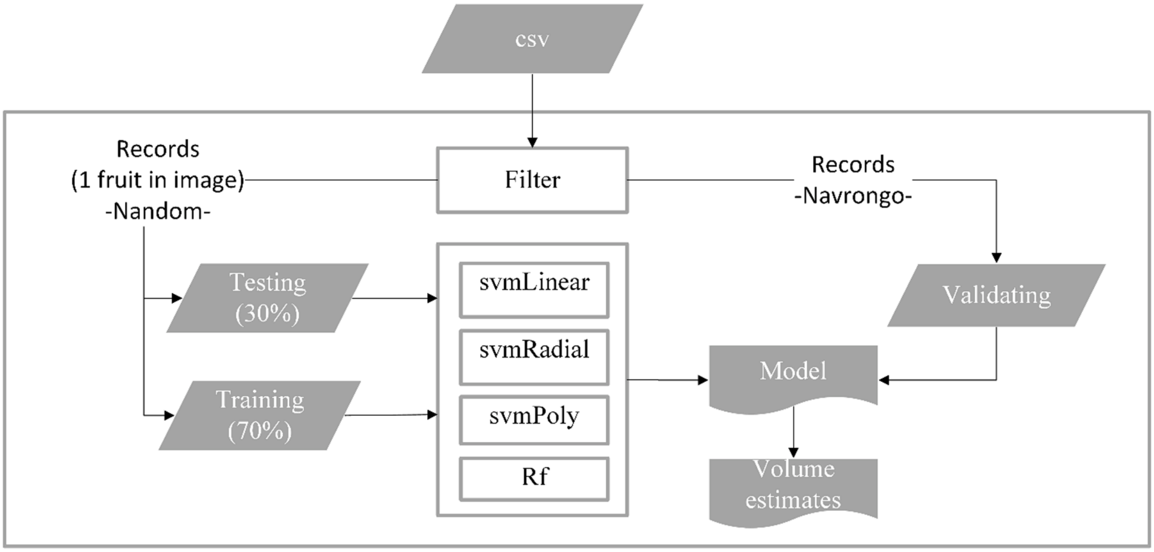

Fig. 5. Training, testing, and validation process for volume quantification using machine learning.

normal probability density functions (PDFs). All the sampling distributions of the means were approximated to a normal distribution for simplicity. The best-fit distributions were used to define the Bayesian prior distribution for the mean (mu) and standard deviation (sigma). The prior distributions were used as a proxy for expert or industry knowledge of the population distribution of fruits. Arbitrary threshold values were set and used as industry standards to classify fruit mass, volume, or density as either small/low, medium, or large/high.

The process established the posterior distribution from point estimates from the fruit quantification models. The distributions provided insight into the confidence interval of point estimates and the probability of the sample belonging to a class (small/low, medium, or large/high) using the RStan package [28,29] (Fig. 6). The density was estimated as the ratio of mass to volume.

3. Results

3.1. Measurement of fruit characteristics

The samples exhibited a variety of shapes and measured characteristics. The shapes observed were fusiform (36 %), crescent (12 %), ventricose (45 %), and globose (8 %). The volume varied from 150 cm^3 to 1820 cm^3, and the weight varied from 60 g to 640 g. The maximum length and circumference varied from 10 cm to 39 cm and from 18.4 cm to 41 cm, respectively (Table 1).

Table 1
Summary statistics of measured fruit characteristics.

Statistic	Weight (g)	Volume (cm^3)	Max. length (cm)	Circumference (cm)
Min.	60	150	10.0	18.4
1st Qu.	150	423	19.0	24.0
Median	210	620	23.0	27.2
Mean	226	682	23.0	27.3
3rd Qu.	290	880	27.0	30.2
Max.	640	1820	39.0	41.0
Sd	0.109	0.339	5.811	4.535

In general, the data from Nandom presented greater variation than did those from Navrongo. It completely overlapped the range of values from Navrongo with variations in the frequency of occurrence. The distributions of all the observed parameters were skewed (Fig. 7).

The summary statistics of the measurements and densities from the study areas are shown in Table 2. The means of samples from the Nandom Municipality and their standard deviations were mostly greater than those from Navrongo. Despite the greater mean length observed in the Nandom group, the standard deviation was lower than that in the Navrongo group.

Fruit circumference and density from both study areas were normally distributed, and length measurements from Nandom were also

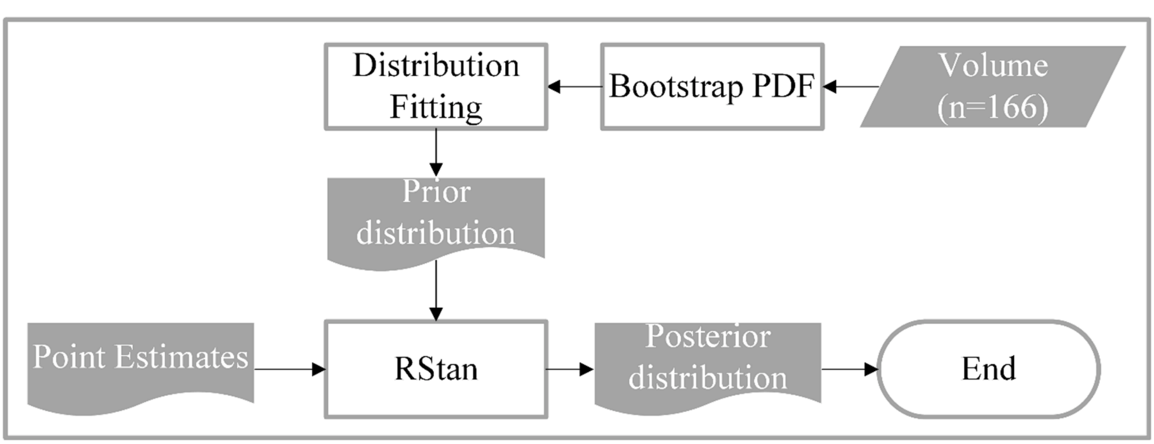

Fig. 6. Volume estimation and distribution modeling from new images.

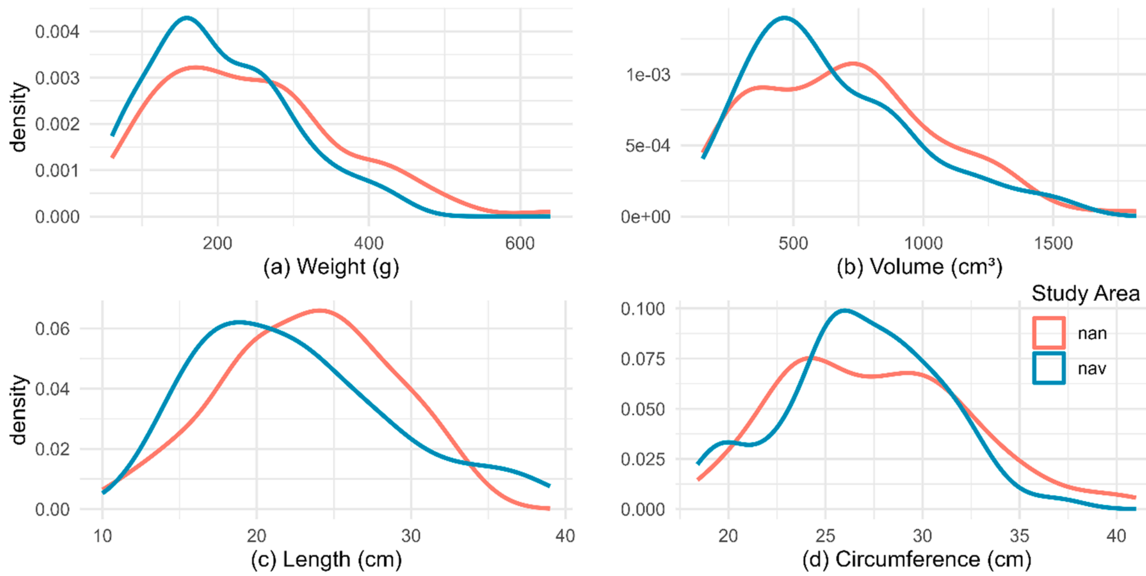

Fig. 7. Distribution of morphological characteristics in samples collected from the Nandom (nan) and Navrongo (nav) study areas.

Table 2
Summary of the means and standard deviations of the measurements and densities from the study areas.

Study area	Variable	Weight (g)	Volume (cm^3)	Length (cm)	Circumference (cm)	Density (g/cm^3)
Nandom	Mean	241.6	707.2	23.240	27.543	2.933
	Std. dev	116.9	349.9	5.444	4.839	0.507
Navrongo	Mean	202.2	643.8	22.555	26.843	3.181
	Sd	91.4	320.5	6.361	4.016	0.480

normally distributed. The mean circumference ($p = 0.314$) was not significantly different between the study areas, but the mean density ($p = 0.002$) was different.

Weight, volume, and length in the Navrongo group were not normally distributed. The medians of weight, volume, and length from Nandom were 230.0 g, 710.0 cm^3 and 23.60 cm, respectively. Their interquartile range (IQR) values were also 0.16, 0.49, and 8.00, respectively. In Navrongo, the corresponding values were 170.0 g, 580.0 cm^3, and 22.00 cm, with IQRs of 0.12, 0.42, and 10.00, respectively. The differences between the medians of volume ($p = 0.265$) and length ($p = 0.178$) were not statistically significant. However, the between-weight ($p = 0.037$) differences were significant. The differences observed can be attributed to factors influenced by the climate gradient.

3.1.1. *Fruit detection and image feature extraction*

The training process went through 3000 iterations with loss box regression, loss classification, and loss mask values of 0.061, 0.015, and 0.052, respectively. The losses (box regression, classification, and mask) decreased as the model progressively learned and improved its performance on the detection and segmentation tasks. The mask accuracy was 97.77 %, which also indicated that the model was proficient at accurately segmenting the pixels of the baobab fruit.

The two-dimensional (2D) image characteristics extracted from the segmented fruit regions exhibited substantial diversity. The pixel count difference for the equivalent diameter (Eq. Diameter) was approximately 30 pixels compared with approximately 394,232 for the bounding box area (Bb. Area). Parameters such as the major diameter displayed a more concentrated distribution, whereas the others exhibited greater diversity, highlighting heterogeneity within the dataset (Appendix, Table A1).

3.2. *Quantification of volume from extracted image features*

Overall, the best and most stable model during training was the random forest model, with an RMSE, R^2, and MAE of 15.80, 99.8 %, and 8.47, respectively. The accuracy metrics of svmLinear were the worst. The other models displayed moderate values during training. A similar pattern was observed during testing, where Random Forest was the best performing model and svmLinear was the worst. In the testing dataset, the svmRadial and svmPoly flipped performance positions when compared to their training positions. Generally, there was a small decrease in performance from training to testing (Appendix Table A2).

In the validation dataset, the svmPoly model was best and closely matched by svmLinear in terms of the R^2 value. In addition, the svmLinear model yielded the best RMSE and MAE values. On the other hand, the RF model displayed a balanced combination of RMSE, R^2, and MAE values. The svmRadial model showed the worst performance in terms of all the metrics (Appendix Table A3).

A plot of the estimated volumes of single fruits against those observed by the water displacement method from the validation dataset summarizes the performance of the models. The plotted points were closely aligned to the 1:1 line, indicating accuracy in estimation except for svmRadial, which deviated, and svmPoly, which appeared to consistently underestimate the fruit volume (Fig. 8).

3.2.1. *Statistical analysis*

The mean difference between volume approximations from each of the svmPoly, svmLinear, and random forest models and the water displacement method (WDM) was not statistically significant ($P \geq 0.05$), except for svmRadial ($P = 0.01$).

The Bland–Altman plots in Fig. 9 show that the differences in volumes estimated by the model and those estimated by the WDM were normally distributed. The 95 % of the volume differences are expected to lie between the dotted lines (95 % limits of agreement). The volume

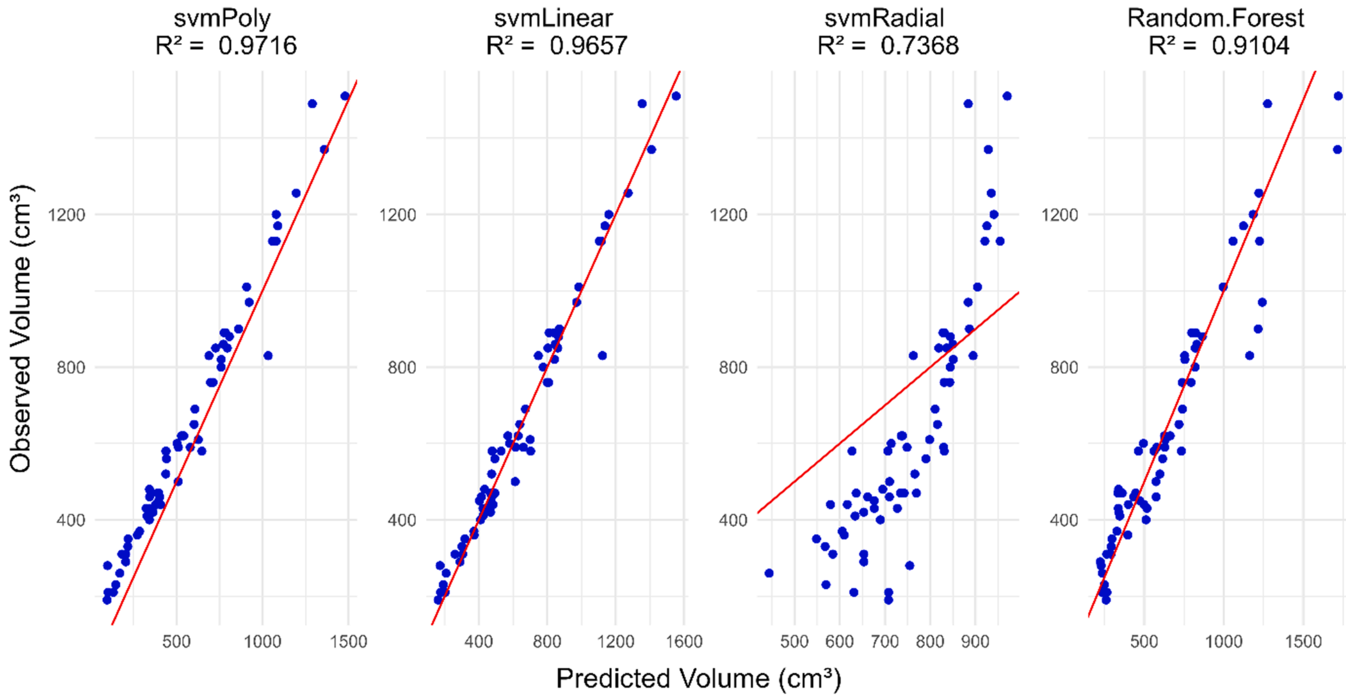

Fig. 8. Regression of the observed (WDM) volume from Navrongo on the predicted volume from machine learning models.

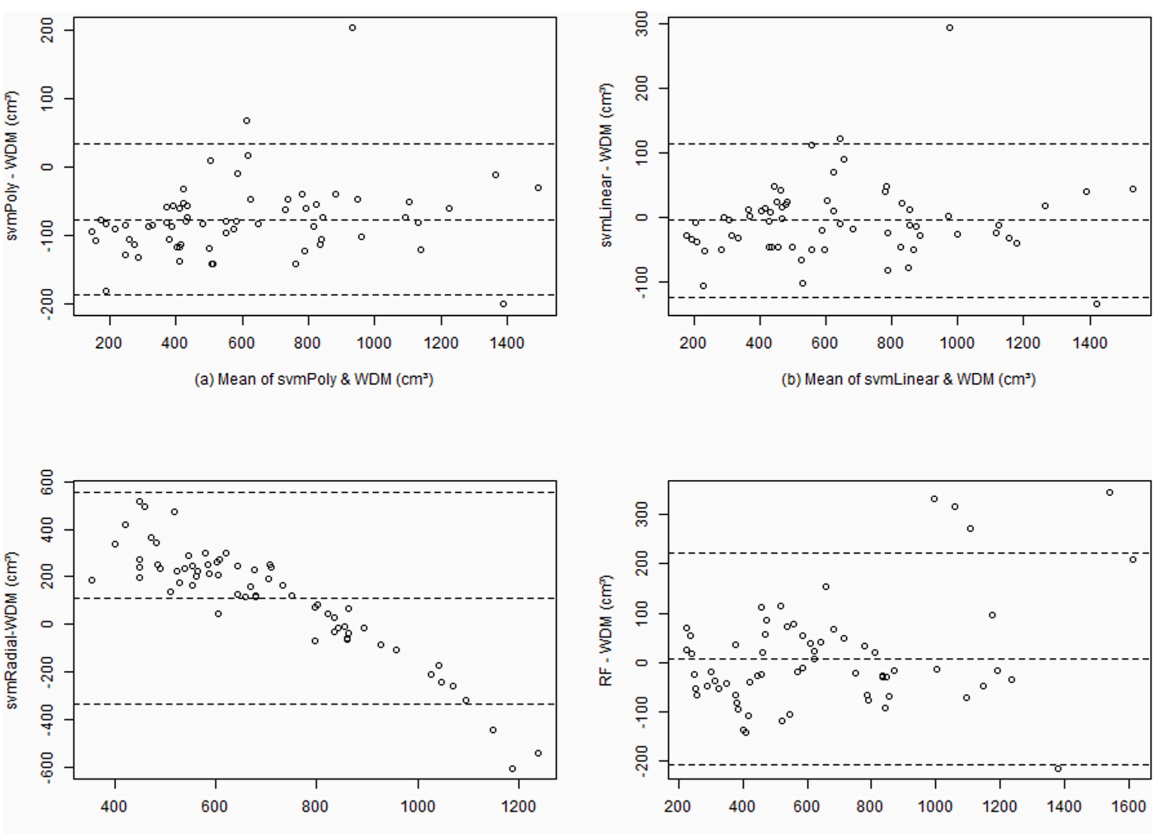

Fig. 9. Bland–Altman plot for the comparison of volumes estimated by machine learning models and the water displacement method (WDM); the outer lines indicate the 95 % limits of agreement, and the centerline shows the average difference.

differences between the model quantifications and WDM can be seen in Fig. 9a–d. The differences were normally distributed for svmLinear (Fig. 9a), svmPoly (Fig. 9b), and random forest (Fig. 9d).

Fig. 9c shows that for small baobab fruits, the volume estimated by the svmRadial method was greater than that estimated by the WDM, and vice versa. Thus, the model overestimates the volume of small fruits and understates large fruits. This may be because the relationship between the extracted image features and the volume is nonlinear.

3.2.2. Important image features for volume determination

The area of the segmented fruit region and the equivalent diameter were the dominant variables, contributing nearly 100 % of the variance explained by the SVM models. All other features contributed less than 80 %. The major diameter contributed 68.25 %. Positional features were mostly inconsequential or of very small importance.

In the random forest model, the major diameter was the most important variable, contributing nearly 100 % of the variance explained. The area of the segmented fruit region and the equivalent diameter were not very useful variables, as they had less than 40 % explanatory power.

3.3. Single variable mass regression modeling

Fig. 10(a) shows a scatter plot of the observed mass against volume. A quadratic relationship was observed between mass (g) and volume (cm^3), with an intercept of 38.23, a slope of 0.25, a coefficient of the quadratic term of 4.49×10^{-5}, and an adjusted R^2 of 92 %. The predicted mass was further regressed against the observed mass (Fig. 10(b)). The values were randomly clustered along the 1:1 line with gradient 1 and intercept 0.

3.4. Modeling probability density functions

The prior probability density functions (PDFs) of the sampling distribution of 1 million bootstrapped means of mass and volume were gamma-distributed, but density was log-normally distributed. The distributions of the standard deviations were gamma, normal, and log-normal for mass, volume, and density, respectively (Appendix, Table A4).

The Rhat ($\check{R}$) values computed for all the models were unity, indicating convergence of the Monte Carlo Markov chain sampling process. The autocorrelation decreased with increasing lag to values close to zero at a lag of approximately five for the samples. In addition, there was a strong central tendency with randomly distributed aberrations that did not depict any trend or distinctions between individual chains.

In Fig. 11, the posterior distributions are shown in red, and the industry distribution is shown in blue. The plot shows that the majority of fruits collected from Nandom were collected from a population with an average mass of 218.87 ± 7.00 g and a standard deviation of 8.04 ± 0.42 g. The posterior distribution of volume followed a distribution similar to that of the population. It had a mean value of 671.39 ± 22.03 cm^3 and a standard deviation of 25.84 ± 1.25 cm^3. On the other hand, the distribution of density further decreased compared with that observed for mass and density. It had a mean value of 0.33 ± 0.00 g/cm^3 and a standard deviation of 0.004 ± 0.00 g/cm^3 (Fig. 11).

The probability below the lower threshold was the highest in the density distribution and the lowest in the volume distribution. The situation reverses between the thresholds. Beyond the upper threshold, the probabilities decreased from mass to volume to density (Table 3).

4. Discussion

4.1. Measurement of fruit characteristics

The fruit samples from Nandom exhibited greater variability in fruit mass than those from Navrongo, but all values observed in Navrongo were within the range observed in Nandom. Similar wide ranges were observed for Mali and Malawi in western and southeastern Africa [9]. The average fruit mass in this study was slightly greater than that in Mali and Malawi, but the range covered the intervals documented in earlier studies [6,30]. The slight differences observed in the means across studies did not suggest that the samples could be from different populations.

Fruit size or volume is often represented by the maximum diameter or fruit length [9]. On the African continent, the ranges of fruit length and width are 7.5–54 cm and 7.5–20 cm, respectively [6]. The wide difference between the minimum and maximum length and width is consistent with the variability in volume in this study and provides a basis for the wide application of the algorithms derived. However, these algorithms cannot be applied universally since the samples may not be representative of all the baobabs on the market.

4.2. Estimation of volume from extracted image features

In the study conducted by Omid et al. [31], computer vision and image processing techniques were utilized to estimate fruit volume, resulting in R^2 values of 96.2 % for lemons, 97.0 % for limes, 98.5 % for oranges, and 95.9 % for tangerines. These R^2 values were indicators of the goodness of fit for their volume estimation models. The results from the random forest model in this study outperformed them, with an R^2 value of 99.8 % in training. Contrary to the findings of Fitriyah [12], this study demonstrates that it is possible to obtain good accuracy of volume estimates using single-view images of fruits with non-axis-symmetric

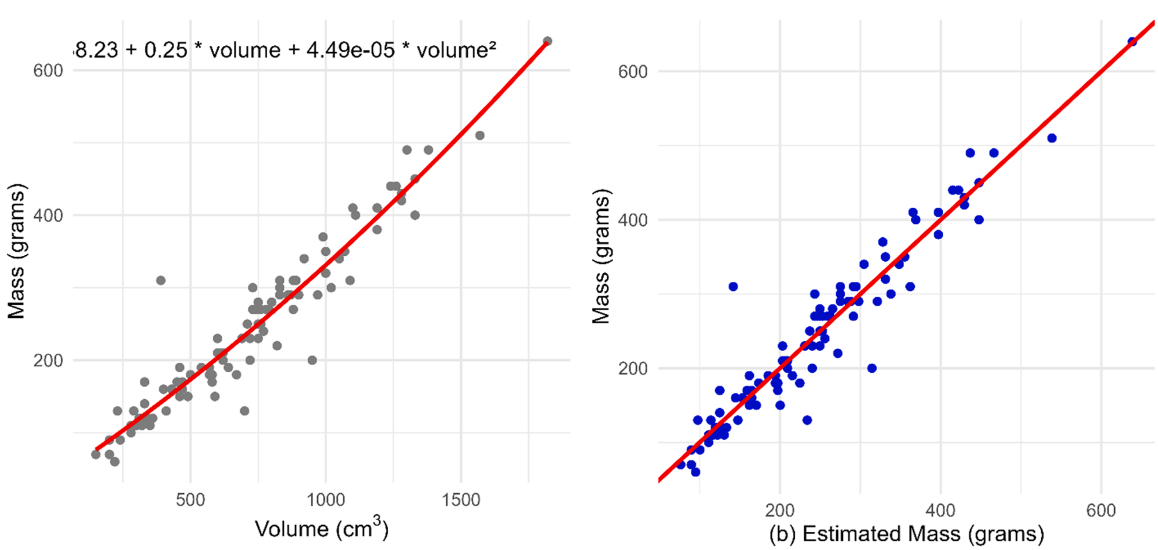

Fig. 10. (a). Regression of observed mass to volume, mass = 38.23 + 0.25 × volume + 4.49e−05 × volume^2, R^2= 92 % and (b) scatter plot of observed mass to estimated mass around the 1:1 line.

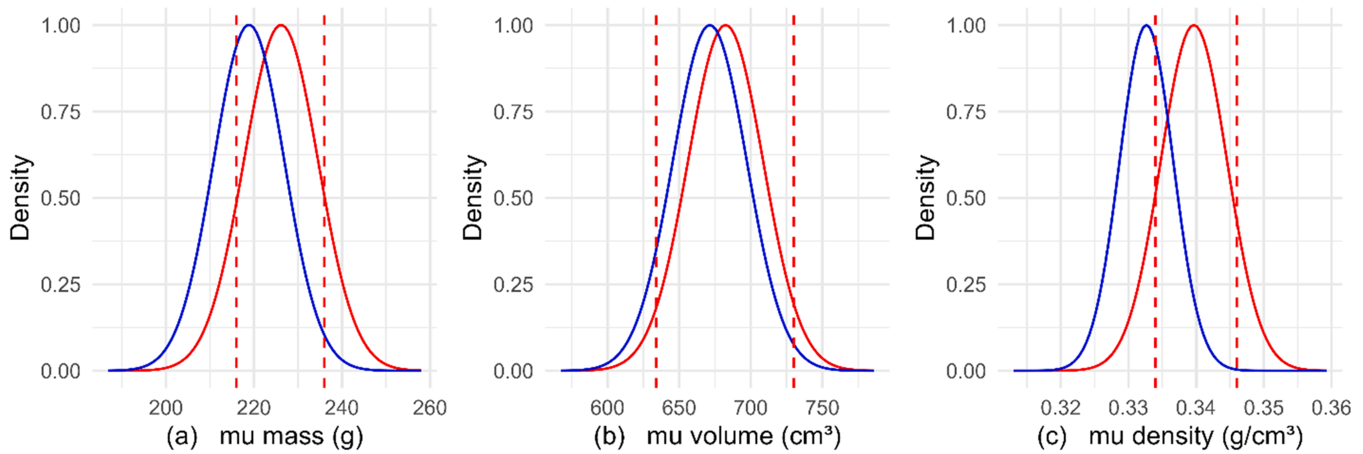

Fig. 11. Comparison of prior (red) and posterior (blue) population distributions of samples obtained from Nandom.

Table 3
Cumulative probability below, between, and above the threshold for mass, volume, and density posterior distributions.

Probability	Mass (g)	Volume (cm^3)	Density (g/cm^3)
Below min threshold	0.39 ± 0.26	0.13 ± 0.16	0.60 ± 0.28
Between max-min threshold	0.55 ± 0.21	0.82 ± 0.15	0.39 ± 0.26
Above max threshold	0.05 ± 0.09	0.04 ± 0.08	0.01 ± 0.03

shapes. Nyalala et al. [19] reported that combining both 2D and 3D image feature variables leads to better predictions of fruit volume than using only 2D feature variables. However, 2D models have the advantages of being simpler and requiring less time and computational resources.

In this study, the volumes predicted by the svmRadial model consistently either underestimated or overestimated the volume, depending on the fruit size. Relying on them for decision-making could result in financial losses, pricing errors, and inefficiencies in resource allocation and supply chain operations.

4.2.1. Important image features for volume determination

Compared with positional features, 2D geometric features are useful estimators of baobab fruit volume. The major diameter is the most useful for the random forest and variants of the support vector machines. The area of the segmented region and equivalent diameter are better alternatives to the major diameter when considering support vector machine models alone.

Previous studies have focused on using 2-dimensional image features such as the projection area, perimeter, eccentricity, major-axis length, minor-axis length, radial distance, horizontal length of the bounding box, and vertical length of the bounding box to estimate volume via regression [12,19]. Despite the successes achieved, emphasis has mostly been placed on axis-symmetric fruits. The equivalent diameter introduced in this study and shown to be relevant in regression by support vector machines provides an interesting basis for further study of the volume of axis nonsymmetric fruits [19].

4.3. Single-variable mass regression model

In certain production, marketing, or research settings, mass may be a preferred measurement. To convert directly measured volumes and estimates obtained from machine learning models to corresponding mass values, a univariate relationship between mass and volume is appropriate.

4.4. Modeling probability density functions

Fruit size distribution is important for sorting and grading fruits. In the baobab fruit industry, fruit size is linked to sweetness, consumer preferences, and market value [5,6]. The weight and proportion of pulp are also taken into account when grading baobab fruits [32]. According to a study by Venter and Witkowski [33], larger fruits contain more seeds and pulp, and sorting by size can lead to more accurate predictions. In their study, they used fruit length and diameter as indicators to categorize mature baobab fruits into small, medium, and large sizes. However, this can be a complex approach, as it relies on a combination of indicators.

This study presents a method that involves computing cumulative probabilities based on the distribution of physical properties, such as mass, volume, and density. By using observable physical properties, it becomes easier to establish size thresholds and sort baobab fruits into small, medium, and large sizes. The model is effective at sampling from the posterior distribution.

Optimizing storage and transportation planning for the baobab fruit industry requires knowledge of its physical properties and distribution. By sorting fruits into different size categories based on observable physical properties, sellers can offer standardized size categories to buyers, providing transparency and consistency in product offerings. Buyers can make informed decisions on the basis of their specific requirements or preferences regarding fruit size. Using this model in supply chain management processes can lead to overall optimization, from storage to transportation to sales. A clear understanding of baobab fruit sizes based on physical properties allows for streamlined operations, reduced costs, and improved customer satisfaction.

5. Conclusion and recommendations

This study provides insights into the morphological characteristics of baobab fruits across the study area. The morphological characteristics of baobab fruits from Nandom are greater than those from Navrongo, indicating the impact of environmental factors on fruit morphology.

It has further established that computer vision combined with machine learning techniques, specifically random forest and support vector machine algorithms, can efficiently quantify fruit volume from 2D image characteristics such as the major diameter, area of the segmented fruit region, and equivalent diameter. The equivalent diameter of the segmented fruit region introduced in this study is a good predictor variable of fruit volume in support vector machines. Computer vision can detect baobab fruit from an image with 97.77 % accuracy, and the random forest model can quantify the volume with an R^2 value of 99.8 %, suggesting that models built solely on 2D image features can be a viable alternative for measuring fruit volume. Additionally, the study established a quadratic relationship between mass and volume, with an R^2 of 92 %.

The point estimates from computer vision and machine learning models can be extended by detecting the posterior distribution of the samples under study to provide valuable insights that can optimize sorting, transportation planning, storage, and market pricing strategies.

Commercial companies producing baobab powder and seed oil should apply these models for effective production planning. To enhance the model, further research is recommended to understand the effects of climate gradients on baobab fruit morphology.

Overall, this study contributes to our understanding of baobab fruit morphology and highlights the potential of artificial intelligence methods and distribution modeling in ecological research and agricultural management. The findings presented pave the way for future studies aimed at improving fruit quantification and management planning in the agricultural sector.

Funding information

This work is funded by the Ministry of Foreign Affairs of Denmark and administered by the Danida Fellowship Centre through the Climate Change Resilience of Ecosystem Services (CRES) Project with Grant No. DFC File No. 20-13-GHA.

CRediT authorship contribution statement

Franklin X. Dono: Writing – original draft, Methodology, Investigation, Formal analysis, Conceptualization. **Bernard N. Baatuuwie:** Writing – review & editing, Supervision, Methodology, Conceptualization. **Felix K. Abagale:** Writing – review & editing, Supervision, Methodology, Conceptualization. **Peter Borgen Sørensen:** Writing – review & editing, Supervision, Methodology, Conceptualization.

Declaration of competing interest

The authors declare that they have no conflicts of interest.

Data availability

Data will be made available on request.

Acknowledgments

The authors thank the West African Centre for Water, Irrigation and Sustainable Agriculture (WACWISA) and the University for Development Studies, Ghana, for providing the necessary support to conduct this study.

Appendix

Table A1
Summary statistics of the extracted image characteristics for mass determination.

Statistic	Area (pixels)	Eq. diameter (pixels)	Mj. diameter (pixels)	Bb. area (pixels)
Min.	47,853.00	45.04	353.70	63,099.00
1st Qu.	85,491.50	54.66	539.37	124,088.75
Median	119,453.00	61.10	637.89	177,727.00
Mean	120,299.22	60.39	641.62	181,674.66
3rd Qu.	149,223.75	65.81	749.59	226,137.50
Max.	229,970.00	76.01	1039.91	457,331.00

Table A2
Comparative performance of ML volume models on training and testing data—unveiling insights into RMSE, *R*-squared, and MAE metrics.

Model	TRAINING			TESTING		
	RMSE	*R*-squared	MAE	RMSE	*R*-squared	MAE
Random Forest	15.796	0.998	8.465	50.819	0.980	22.988
svmRadial	56.396	0.973	37.894	70.961	0.961	46.967
svmPoly	59.657	0.970	41.152	69.157	0.962	43.366
svmLinear	65.770	0.964	45.311	72.456	0.958	47.666

Table A3
Comparative performance of ML volume models on single fruit image features from Navrongo data—unveiling insights into RMSE, *R*-squared, and MAE metrics.

Model	RMSE	R-squared	MAE
svmPoly	95.24137	0.9716203	86.10354
svmLinear	60.18458	0.9657215	41.32424
Random Forest	108.80602	0.9103636	78.20715
svmRadial	251.34992	0.7367830	211.48176

Table A4
Prior distribution of parameters used in the Stan.

Data	Parameter	PDF	Approximation
Mass	Mean	Gamma (717.75, 3.17)	Normal (266.15, 8.44)
	Sd	Gamma (268.10, 2.47)	–
Volume	Mean	Gamma (676.25, 990.98)	Normal (682.40, 26.24)
	Sd	Normal (337.66, 18.61)	–
Density	Mean	Lognormal (−1.08, 0.01)	Normal (0.340, 0.005)
	Sd	Lognormal (−2.79, 0.16)	–

References

[1] J. Gebauer, E. Luedeling, A note on baobab (*Adansonia digitata* L.) in Kordofan, Sudan, Genet. Resour. Crop. Evol. 60 (4) (2013) 1587–1596, https://doi.org/10.1007/s10722-013-9964-5.

[2] R. Hyde, S. Hartley, K. Millar, European novel foods policy at a critical juncture: drawing lessons for future novel food governance through a retrospective examination of regulation 258/97, Food Drug Law J. 72 (3) (2017) 472–505.

[3] L. Welford, G. Le Breton, Bridging the gap: phytotrade Africa's experience of the certification of natural products, For. Trees Livelihoods 18 (1) (2008) 69–79, https://doi.org/10.1080/14728028.2008.9752618.

[4] EC, Commission decision: authorizing the placing on the market of baobab dried fruit pulp as a novel food ingredient under regulation (EC) No 258/97 of the European Parliament and of the Council, Off. J. Eur. Union 183 (2008) 38–39.

[5] D.A. Odoom, Characterization of baobab (*Adansonia digitata* L.) in the Builsa District of Ghana, J. Food Technol. Preserv. 2 (1) (2021), https://doi.org/10.36266/JFTP/116.

[6] N.A. Gurashi, M.A. Kordofani, Morphological variation in fruit shapes of *Adansonia digitata* L. from Blue Nile and North Kordofan States, Sudan, J. For. Prod. Ind. 3 (2) (2014) 106–111.

[7] K.F. Egbadzor, Studies on baobab diversity, seed germination and early growth, S. Afr. J. Bot. 133 (2020) 178–183, https://doi.org/10.1016/j.sajb.2020.07.024.

[8] C. Parkouda, H. Sanou, A. Tougiani, A. Korbo, D.S. Nielsen, K. Tano-Debrah, A. Ræbild, B. Diawara, J.S. Jensen, Variability of baobab (*Adansonia digitata* L.) fruits' physical characteristics and nutrient content in the West African Sahel, Agrofor. Syst. 85 (3) (2012) 455–463, https://doi.org/10.1007/s10457-011-9406-3.

[9] A.C. Sanchez, S. De Smedt, N. Haq, R. Samson, Comparative study on baobab fruit morphological variation between western and south–eastern Africa: opportunities for domestication, Genet. Resour. Crop Evol. 58 (8) (2011) 1143–1156, https://doi.org/10.1007/s10722-010-9647-4.

[10] G.N. Gouwakinnou, A.E. Assogbadjo, A.M. Lykke, B. Sinsin, Phenotypic variations in fruits and selection potential in *Sclerocarya birrea* subsp. birrea, Sci. Hortic. 129 (4) (2011) 777–783, https://doi.org/10.1016/j.scienta.2011.05.041.

[11] I. Mkwezalamba, C.R.Y. Munthali, E. Missanjo, Phenotypic variation in fruit morphology among provenances of *Sclerocarya birrea* (A. Rich.) Hochst, Int. J. For. Res. 2015 (2015) 1–8, https://doi.org/10.1155/2015/735418.

[12] H. Fitriyah, Accuracy of various methods to estimate volume and weight of symmetrical and non-symmetrical fruits using computer vision, J. ICT Res. Appl. 16 (3) (2022) 210–225, https://doi.org/10.5614/itbj.ict.res.appl.2022.16.3.2.

[13] Ifmalinda, R.E. Putri, I. Rasinta, Estimation of size, volume and weight of oranges using digital images processing, IOP Conf. Ser.: Earth Environ. Sci. 1059 (1) (2022), https://doi.org/10.1088/1755-1315/1059/1/012016.

[14] I. Nyalala, C. Okinda, Q. Chao, P. Mecha, T. Korohou, Z. Yi, S. Nyalala, Z. Jiayu, L. Chao, C. Kunjie, Weight and volume estimation of single and occluded tomatoes using machine vision, Int. J. Food Prop. 24 (1) (2021) 818–832, https://doi.org/10.1080/10942912.2021.1933024.

[15] A.B. Koc, Determination of watermelon volume using ellipsoid approximation and image processing, Postharvest Biol. Technol. 45 (3) (2007) 366–371, https://doi.org/10.1016/j.postharvbio.2007.03.010.

[16] C. Zheng, T. Liu, A. Abd-Elrahman, V.M. Whitaker, B. Wilkinson, Object-detection from multi-view remote sensing images: a case study of fruit and flower detection and counting on a central Florida strawberry farm, Int. J. Appl. Earth Obs. Geoinform. 123 (August) (2023) 103457, https://doi.org/10.1016/j.jag.2023.103457.

[17] K. Kheiralipour, A. Kazemi, A new method to determine morphological properties of fruits and vegetables by image processing technique and nonlinear multivariate modeling, Int. J. Food Prop. 23 (1) (2020) 368–374, https://doi.org/10.1080/10942912.2020.1729177.

[18] L. Raja Sekar, N. Ambika, V. D, T. K, Fruit classification system using computer vision: a review, Int. J. Trend Res. Dev. 5 (1) (2018) 2394–9333. www.ijtrd.com.

[19] I. Nyalala, C. Okinda, L. Nyalala, N. Makange, Q. Chao, L. Chao, K. Yousaf, K. Chen, Tomato volume and mass estimation using computer vision and machine learning algorithms: cherry tomato model, J. Food Eng. 263 (July) (2019) 288–298, https://doi.org/10.1016/j.jfoodeng.2019.07.012.

[20] S.M. Mansuri, P.V. Gautam, D. Jain, C. Nickhil, Pramendra, Computer vision model for estimating the mass and volume of freshly harvested Thai apple ber (*Ziziphus mauritiana* L.) and its variation with storage days, Sci. Hortic. 305 (2022) 111436, https://doi.org/10.1016/j.scienta.2022.111436.

[21] J. Siswantoro, A.S. Prabuwono, A. Abdulah, Volume measurement of food product with irregular shape using computer vision and monte carlo method: a framework, Procedia Technol. 11 (Iceei) (2013) 764–770, https://doi.org/10.1016/j.protcy.2013.12.256.

[22] M. Khojastehnazhand, M. Omid, A. Tabatabaeefar, Determination of tangerine volume using image processing methods, Int. J. Food Prop. 13 (4) (2010) 760–770, https://doi.org/10.1080/10942910902894062.

[23] Ministry of Food and Agriculture (MOFA) Ghana, Savannah Agriculture Value Chain Development Project (SADP)-Nandom Municipality: Environmental and Social Impact Assessment (ESIA), SAL Consult Limited, P. O. Box GP20200, Accra, Ghana, 2022. June.

[24] D.O. Gray, A.R. Hayman, *Adansonia digitata* - African baobab, Phytochemistry 26 (3) (1986) 839–841.

[25] A. Dutta, A. Zisserman, The VIA annotation software for images, audio and video. MM 2019 - Proceedings of the 27th ACM International Conference on Multimedia, 2019, pp. 2276–2279, https://doi.org/10.1145/3343031.3350535.

[26] T.Y. Lin, et al., Microsoft COCO: common objects in context. Lecture Notes in Computer Science LNCS, in: European Conference on Computer Vision, PART 5, vol. 8693, 2014, pp. 740–755, https://doi.org/10.1007/978-3-319-10602-1_48.

[27] J.M. Bland, D.G. Altman, Measuring agreement in method comparison studies, Stat. Methods Med. Res. 8 (2) (1999) 135–160, https://doi.org/10.1177/096228029900800204.

[28] M.D. Hoffman, A. Gelman, The no-U-turn sampler: adaptively setting path lengths in Hamiltonian Monte Carlo, J. Mach. Learn. Res. 15 (2008) (2014) 1593–1623.

[29] Stan Development Team. (2024). *{RStan}: the {R} interface to {Stan}*. https://mc-stan.org/.

[30] C.R.Y. Munthali, P.W. Chirwa, F.K. Akinnifesi, Phenotypic variation in fruit and seed morphology of *Adansonia digitata* L. (Baobab) in five selected wild populations in Malawi, Agrofor. Syst. 85 (2) (2012) 279–290, https://doi.org/10.1007/s10457-012-9500-1.

[31] M. Omid, M. Khojastehnazhand, A. Tabatabaeefar, Estimating volume and mass of citrus fruits by image processing technique, J. Food Eng. 100 (2) (2010) 315–321, https://doi.org/10.1016/j.jfoodeng.2010.04.015.

[32] M. Omondi, F.K. Rimberia, C.M. Wainaina, J.B.N. Mukundi, J. Orina, J. Gebauer, K. Kehlenbeck, Fruit morphological diversity and productivity of baobab (*Adansonia digitata L.*) in coastal and lower eastern Kenya, For. Trees Livelihoods 28 (4) (2019) 266–280, https://doi.org/10.1080/14728028.2019.1659861.

[33] S.M. Venter, E.T.F. Witkowski, Baobab (*Adansonia digitata* L.) fruit production in communal and conservation land-use types in Southern Africa, For. Ecol. Manag. 261 (3) (2011) 630–639, https://doi.org/10.1016/j.foreco.2010.11.017.